Automation in Construction
2018-03-02

Optimal Control of Wheel Loader Actuators in Gravel Applications

Bobbie Frank[1,2], Jan Kleinert[3], Reno Filla[2]
[1]Lund University, faculty of engineering, Box 118 S-221 00 Lund, Sweden.
[2]Volvo Construction Equipment, SE-631 85 Eskilstuna, Sweden.
[3]Fraunhofer-Institut für Techno- und Wirtschaftsmathematik ITWM, Fraunhofer-Platz 1, 67663 Kaiserslautern
bobbie.frank@volvo.com, jan.kleinert@dlr.de, reno.filla@volvo.com

Corresponding author:
Bobbie Frank
TCA11, SE-631 85 Eskilstuna, Sweden
Telephone: +46-16-5414475
E-mail: bobbie.frank@volvo.com

1 Abstract

The paper is about finding the global optimum for a wheel loader work cycle in a gravel application. This includes simulating the gravel and extracting the trajectories for the main actuators; propulsion, lift and tilt, during the work cycle. The optimal control method is dynamic programming and the optimum is calculated with regard to fuel efficiency [ton/l] but can be weighted towards productivity [ton/h].

The analytical optimal control results are compared to an extensive empirical measurement done on a wheel loader and shows around 15% higher fuel efficiency compared to the highest fuel efficiency measured among real operators.

Keywords: Optimal control, Dynamic programming, Construction machines, Gravel simulation, Wheel loader, Fuel efficiency.

1. Introduction

The wheel loader is considered as one of the most versatile construction equipment machines that perform multiple tasks on work sites. However, in this paper the focus is on a wheel loader working in a bucket application as part of a production chain performing a *"short loading cycle"*. This use case has been chosen for demonstration of the method, due to the fact that this is one of the most common applications for larger wheel loaders. The versatile usage and large variations in operator behavior, due to multiple actuators, make optimizing fuel efficiency [ton/l] and productivity [ton/h] a challenge when designing a wheel loader. The variation due to operator behavior, among experienced operators can be as much as 150% in fuel efficiency and 300% in productivity [1]. Customers who buy construction machines use them as tools to make money as a business; consequently the running costs, such as fuel, maintenance and operator wage, are essential to minimize. Taking economics and environmental care into consideration, it is important to optimize the fuel efficiency [ton/l] and productivity [ton/h] of each construction machine.

The literature contains several studies related to optimization of construction machines and wheel loaders in particular. However these papers have only considered machine speed and lifting during the transport phase [2,3] or only minimized consumed fuel per travelled distance when considering the drive line [4], both of which are great simplifications of the problem. In this paper a method for optimizing the complete work cycle, including the loading phase, is presented. The loading phase is important because about one third of the energy is spent in the gravel pile. This is visible in literature such as [5] where simple performance indicators are used to study fuel efficiency improvement of a complete wheel loader work cycle by optimizing bucket design and bucket filling. The bucket filling phase is also the most difficult part of the cycle for the operator. Optimal driving, for on-road applications, is covered in literature such as [6,7,8,9,10,11] while similar problems are solved for off-road in [2,3,12] and an optimization of a full work cycle in a grapple application of a wheel loader is solved in [13]. In the literature, there is a tendency to simplify the models of the major components to suit the optimization tool chosen. If the problem is non-convex, dynamic programming is the only reasonable method that guarantees global optimum. In this paper, a method is developed based on dynamic programming to ensure that the global optimum is found, with regard to fuel efficiency and productivity. In [14,15,16,17] a global optima has been found, using dynamic programming, to evaluate control strategies, in off-road machines, that need less computational power but do not ensure a global optimum solution for the complete machine as a system. However these papers only consider the primary energy converter side, for example: the internal combustion engine and/or the hydraulic pumps. The method presented in this paper also takes into consideration the actuators and does not rely on a recorded work cycle.

The main research contribution in this paper is to formulate a dynamic programming problem that is able to be able to optimize the actuator movements in a complete work cycle with regard to fuel efficiency at a given productivity, including the three main actuators; propulsion, lift and tilt. This is done with a proven environmental model, to guarantee correct interaction between the gravel pile and bucket, and with models of the wheel loader based on maps of real measurement data of all major components in the wheel loader. The result of the optimization, calculated in Section 5, is then compared to the empirically best work cycle found in an operator deviation measurement study, presented in Section 2.

The optimization in this paper excludes the route optimization, handled in literature such as [2,18,19,20]. In [2] the transport part of the work cycle is optimized, including path planning, with steering, machine velocity and load receiver angle, with more simplified equation based models of the internal components.

Secondary research contributions are that this method is shown to be able to be used in the early phases of research and development when performing concept evaluations between different machine concepts and system optimization of the main components in each concept [21] Using the proposed method overcomes the traditional difficulties in simulating wheel loader efficiency and productivity with ad-hoc rule based algorithms. In [22,23] dynamic programming is used to determine the size of the electrical energy storage in a diesel-electric hybrid machine, while [21] demonstrates how the method presented in this

paper applied to all major subsystems in the complete machine. It was also shown in [24] to be possible to extract from the results of this method, the input required for operator assist systems, automatic functions, and autonomous construction machine control development.

For a complex system such as a wheel loader, solving an optimal control problem, and ensuring the solution is a global optimum, requires thorough knowledge about the system. Without this knowledge it is difficult to choose the most suitable optimal control method. In addition, when modeling the wheel loader, it is difficult to make the correct decision regarding reasonable simplifications and system boundaries. These decisions are often necessary to solve the problem within a reasonable computation time. For this reason an introduction to the wheel loader is given below and some of the largest challenges when simulating and controlling a wheel loader are discussed. The method presented in this paper can be applied in other industries that are facing similar challenges when performing a new machine concept evaluation or developing operator assist functions. Applicable industries are where the machine topology with parallel power flow, material interaction, and machine performance limitations are set by the operator, see Figure 2 and Section 1.2. Industries can be, but are not limited to, i.e. agriculture and forestry. An example is found in [25,26], where dynamic programming is used in the energy optimization of the hydraulic system of forestry equipment. In contrast to the examples in [14,15,16,17,22,23,25,26], in this paper the complete machine is considered.

1.1 Paper outline

In the remaining parts of Section 1 a short background description of the wheel loader and the definition of the wheel loader operation optimization are presented. In Section 2 an empirical study is presented where an empirical best case in regards to fuel efficiency, with an acceptable productivity, is found. In Section 3 the wheel loader configuration, with limitations and boundaries, is presented. The problem formulation is set up in Section 4. In Section 5 the numerical theoretical optimum is calculated. The optimization method, wheel loader and environment simulation models and implementation of the optimization algorithms, with limitations, are presented as well. In Section 6 a comparison analysis is done, investigating the differences between the numerical theoretical optimal solution and the empirical best case found in Section 2. The results are presented in Section 7, followed by a discussion in Section 8 and the conclusions are presented in Section 9.

1.2 Wheel Loader Background

As described in [1,27,28], the wheel loader is a versatile working machine used in a vast variety of applications with different attachments such as bucket, grapple [13], material handling arm, etc.. In this paper, the focus is on wheel loaders that are part of a production chain, in particular, bucket applications. The tasks are most often either loading material from the face of a material pile or a virgin bank, loading materials ranging from blasted rock to clay and natural sand, or re-handling, meaning handling material after the crusher, either to feed the next part in the production chain, to stockpile or to load onto trucks out from site. With each application, the wheel loader's work cycle looks different. The most common work cycles for production chain wheel loaders in bucket applications are the *"short loading cycle"*, also called "V-cycle" or "Y-cycle" in literature such as [29,30], and the "load and carry cycle". The major differences between the two cycles are the transport distance, the initial velocity into the gravel pile and that the need for using all actuators at the same time is more critical in the "*short loading cycle*". A visualization of a "*short loading cycle*", loading blasted rock onto an articulated hauler from face as a part of a production chain, is shown in Figure 1.

Figure 1 – A wheel loader performs a "*short loading cycle*" in blasted rock from face, as a part of a production chain [31].

There are two major differences between the more commonly known and studied optimization of an on-road vehicle and of a wheel loader, that increase the complexity of the system, and hence also the optimization. Firstly, the wheel loader has more actuators, propulsion, lift and tilt, comparing to a

single propulsion actuator in the car, hence the operator is central in the control loop, see Figure 2, meaning that different operator behaviors have a higher impact than in a normal on-road application. This results in more degrees of freedom to optimize in the wheel loader case. Secondly, the interaction with the environment in a car is only the interaction with the ground and air and can be simulated using the vehicle motion equation [32] while in the wheel loader the interaction is more complicated. When filling the bucket all three actuators are working against a gravel pile in a complex power balance, see Figure 2.

The schematic picture of the power flow in a wheel loader in Figure 2 reveals the complexity of the system. There is not only a coupling in the power flow at the combustion engine, which is coupled to the torque converter and the hydraulic pumps, but also at the bucket, where the wheels and cylinders are coupled via the gravel pile in the bucket filling phase. This means that the operator needs to balance the power available from the combustion engine between the two main power consumers, driveline and working hydraulics, at all times. Furthermore, the working hydraulics consists of two main functions, lift and tilt, and a number of support functions, such as steering and auxiliaries.

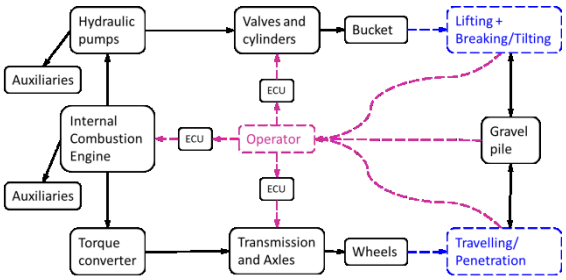

Figure 2 - A schematic picture of the power balance and the control loop in a wheel loader during bucket fill [27,28]. ECU is an on-board computer.

A gravel pile model is necessary to get the correct coupling on the bucket-side of the schematic picture in Figure 2. This can be compared to the rolling resistance in an on-road application but it is responsible for almost all of the fuel consumed in the bucket fill phase, and around one third of the total amount of fuel consumed in a "*short loading cycle*" [33]. The importance of including the gravel pile cannot be emphasized enough.

1.3 Wheel Loader Operation Optimization

When discussing optimizing of the wheel loader operation, regardless if it is targeting fuel efficiency [ton/l] or productivity [ton/h], what often comes to mind is to optimize the wheel loader itself and sometimes also the work cycle layout. However the wheel loader operation optimization is not that simple, resulting in a problem too large to solve at once due to large computational power requirements. A suggestion for sub-dividing the optimization into levels for a wheel loader, working as part of a production chain, is shown in Figure 3.

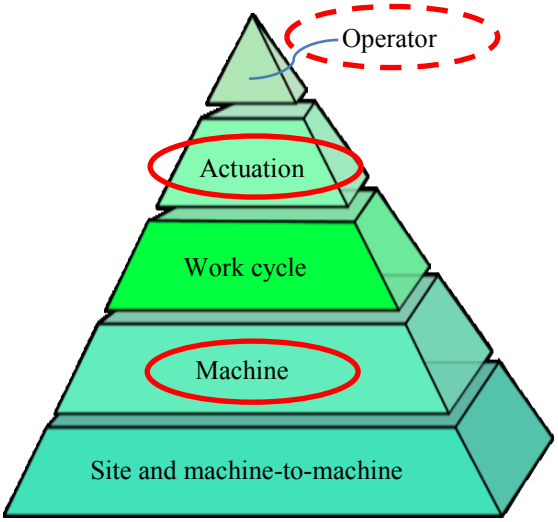

Figure 3 – Suggested optimization levels for a wheel loader, working as part of a production chain. Levels circled in red are targeted in this paper.

The levels are defined as;

Site and machine-to-machine optimization: On a work site, for example a quarry or open pit mine, the fleet of machines and the layout of the site can be optimized with regard to any combination of: energy usage of the complete site, the production rate, initial and/or running costs of the site. This task is further complicated by the imposition of boundary conditions. For example: the contractor has a limited set of machines or the layout of the site has geographical constraints. Once a set of machines has been chosen a continuous optimization has to be performed, with regard to how the machines work together. Optimization at this level is not covered in this paper but rather in literature such as [34,35].

Machine optimization: Given a work task, the wheel loader itself can be optimized, with respect to fuel efficiency and/or productivity. This includes different machine concepts, such as a conventional wheel loader, a diesel-electric hybrid wheel loader, a full electric wheel loader, etc. System optimization, which is the sizing of components such as internal combustion engine, hydraulic

pumps, lifting unit etc. is included as well. Both concept evaluation and system optimization is done by the wheel loader manufacturer. Using the method developed and presented in this paper a concept evaluation and a system optimization can be performed, see [21] for more details.

Work cycle optimization: Given the machine and the work task, there is freedom in how to plan the work cycle. While some boundary conditions, such as the gravel pile position and the load receiver height, may be fixed, there are other boundary conditions that are flexible. This includes the following: load receiver position, turning point of the wheel loader and the position trajectory between the gravel pile, turning point and load receiver. One result of the path planning optimization of the work cycle in [2] is shown in Figure 4. Here the steering angle of the wheel loader together with the x- and y-positions are optimized. The lift is considered only in order to determine that the required height at the load receiver is reached.

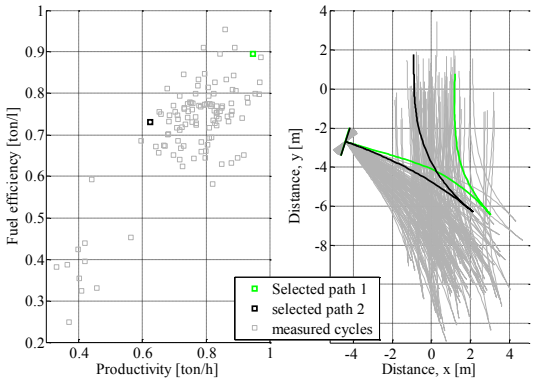

Figure 4 - Left: Normalized values for the recorded productivity from measurements. Right: Recorded Wheel Loader trajectories during measurements. The highlighted trajectories have almost the same travelling distance and bucket load but are different in productivity [2].

The path planning optimization of the work cycle is not covered in this paper but rather in literature such as [2,19,20].

Actuator optimization: Given the work cycle geographical boundary constraints and machine, the cycle can be performed in different ways as regards actuation of the three main actuators; propulsion, lift and tilt. This results in different productivity [ton/h] and fuel efficiency [ton/l]. The method presented in this paper performs the actuator optimization by optimizing; the wheel loader velocity, lift position and tilt position in relation to covered distance by using dynamic programming. The main reason for dividing "*Work cycle optimization*" and "*Actuator optimization*" is to get reasonable computation times.

Operator optimization: This is not really an optimization level if all other levels have been optimized, but is rather about the operator and how to influence how he/she operates the machine. This can be done by operator support systems, automatic functions or autonomous machines. Even if the method presented here will not directly deliver such systems, the results from the optimal control calculations can be used as input when developing them [24], hence the dashed circle in Figure 3. In addition, the "*Work cycle optimization*" will affect the *"Operator optimization"*.

2 The Empirical Study

The main reason for performing the study is to empirically find the best work cycle, with regard to fuel efficiency [ton/l] with an acceptable productivity [ton/h]. The purpose is to validate the calculated numerical theoretical global optimum, presented in Section 5. In an ideal case the number of measured operators would be infinity, or at least all operators in the world, but this is of course not feasible. The secondary reason was to evaluate the usefulness of an operator support tool [1]. The measurement setup presented briefly in this section and further in [1].

Since the theoretical optimization algorithm is designed to cover the "*Actuator optimization*" level in Figure 3, it is important to isolate the same layer in the real world measurements. This was done by ensuring that the environment was the same all the time. For this, the measurement was done indoors to minimize the effect of weather conditions, particularly since the gravel is heavier when moist. Also the same gravel was reused during the whole measurement, and even if the wear of the material was a bit more extensive than expected. In the load and carry application there was more extensive material wear due to wear against the conveyer belt and hopper. In the rock application the material, boulders and shot rock, break apart easier, rounding the edges, which change the material properties. This results in higher uncertainties regarding material wear in these two applications [1]. In the *"Short loading cycle"* the wear was not as big as in the other two application and after analyzing measurement data in conjunction with what had been observed during the measurements the this did

not affect the results much in the *"Short loading cycle"* application. This is also the reason why the indoor, most repetitive application is used as a comparison in this paper. The driving surface was smoothed between all operators to guarantee the same initial condition for all operators. All the measurements were done with the same Volvo L220F wheel loader to ensure that deviation between machines did not affect the results. The work cycle was arranged as in Figure 5. Even though the hauler was placed at the same position in every cycle the turning point in the V-cycle had to be decided by the wheel loader operator. Hence, the difference between the operators will mostly be in the "actuator optimization" layer but also partly in the "work cycle optimization" layer.

Figure 5 – Measurement setup, performing a "Short loading cycle".

In the study, 79 operators operated the wheel loader. Each operator filled 5 haulers, with 3 buckets of gravel in each, resulting in 15 wheel loader work cycles. More about the measurement setup, operator deviation and differences between applications can be found in [1].

2.1 Empirical Study Output

As a first step in the analysis of the empirical study, the average fuel efficiency and productivity for each operator is calculated. Only the wheel loader cycle is included, the hauler cycle when the wheel loader is not doing any work is excluded. As a second step the fuel efficiency and productivity per cycle is calculated. Worth noticing here is the difference between cycle #1, #2 and #3 when filling the hauler. Positioning often takes longer time in the first cycle due to repositioning of the wheel loader to the new pile geometry. This is because the same gravel is used in the test and the hauler does not empty in the exact same spot, see Figure 5. In the third cycle, care has to be taken when emptying the bucket because the hauler is filling up. The second cycle is usually the quickest one with the highest productivity [ton/h] and fuel efficiency [ton/h]. To favor consistently high fuel efficient behavior, the operator with highest average fuel efficiency, that also had a small deviation between the cycles, was chosen, EP15 in this case, and this operator's best cycle, see the green square marker in Figure 6, is used as the benchmark to the numerical theoretical optimum. To be able to use a measured cycle as benchmark the cycle time, turning point and position of hauler and gravel pile are fed into the optimization algorithm. This corresponds to the "*Work cycle optimization*" layer in Figure 3. The output from the optimization algorithm is the movement of the three actuators: lift, tilt and propulsion. This corresponds to the "*Actuator optimization*" layer in Figure 3.

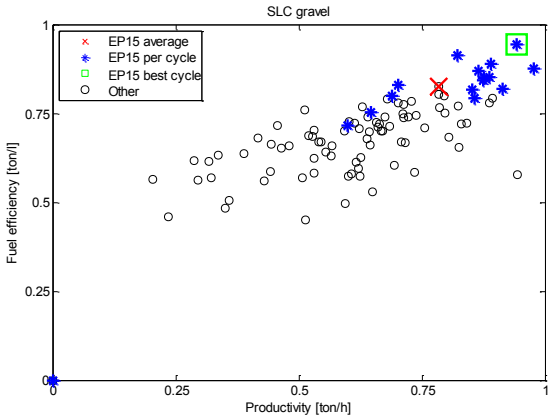

Figure 6 - The fuel efficiency and productivity distribution of the most fuel efficient operator, EP15, compared to the other operators' average. SLC means "short loading cycle". Normalized axes due to Volvo internal results.

Using the input from the measurements in this way will allow the isolation of the "*actuator optimization*" layer in Figure 3, and consequently verify that the optimization result returned is a global optimum. The "*work cycle optimization*" layer is not targeted but rather handled in [2,19,20]. This means that the work cycle parameters, such as turning point, fill position and empty position, both regarding the ground plane, the lift height, the bucket angle and cycle time are set from the measured operator's work cycle.

3 System Setup

The wheel loader concept chosen to demonstrate the methodology presented in this paper is a precursor [36] to the recently revealed concept wheel loader "LX1" [37], performing a *"short loading cycle"* in a production chain, bucket

application. This is a full series hybrid with all three actuators; propulsion, lift and tilt, decoupled. The series hybrid drivetrain consists of one propulsion electric machine and a three speed gearbox without a torque converter. The working hydraulics is also hybridized in series, where one electrical machine propels one hydraulic pump for each function. In this case, lift and tilt are the hydraulic functions accounted for. The steering is not accounted for because the steering must always receive the power needed to steer for reasons of to safety. This means that the problem to be solved has three control signals; lift, tilt and propulsion, see the schematic picture in Figure 7.

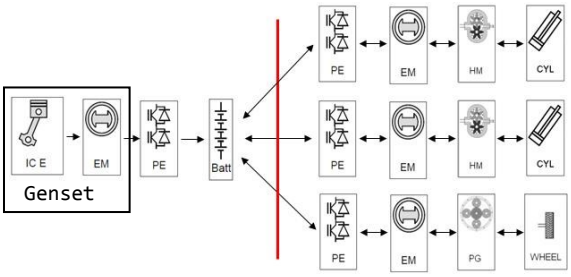

Figure 7 – Schematic picture of the wheel loader concept investigated. ***Schematic picture of the wheel loader concept investigated. The genset is the internal combustion engine and electrical machine on the primary energy converter side. ICE is the internal combustion engine, EM is the electrical machine, PE is the power electronics, Batt is the electrical energy storage (battery or super capacitor), HM is the hydraulic machine, CYL is the hydraulic cylinder actuating lift and tilt, and PG is planetary gears in the axles and hubs.***

The primary energy conversion, the genset and battery, on the left-hand side in Figure 7, are optimized in a separate dynamic programming optimization. This is done to reduce the number of states so that the optimization can be done within a reasonable computational time. To divide the problem into actuation optimization and the primary energy conversion optimization, with the actuator optimization as input to the primary energy conversion optimization, is a reasonable simplification, due to the decoupled nature of the series hybrid system. The limitation of the total power output from the internal combustion engine and energy storage system are included in such a way that the total power of the actuators are not allowed to exceed this limit. Hence, prioritization between the actuators has to be done as well. Because the operator is not involved in the optimization of the primary energy conversion in a series hybrid, and since the optimization result is to be compared with real operator data, the comparison will be at actuator level. Hence no more focus is put on the primary energy conversion optimization in this paper. In [21] a concept evaluation and system optimization is done with complete machine optimization, including producers, on three different wheel loader concepts.

Due to the fact that only the "*actuator optimization*" layer is targeted in the optimal control algorithm and not the "*work cycle optimization*" layer the lack of steering will not affect the resulting trajectories of the actuators but will only significantly reduce the computation time.

4 Problem Formulation

The problem to be solved is to find a global optimum regarding fuel efficiency, at a given productivity, as described earlier. Discrete power loss maps for all components in the machine are used, originating from test rig measurements, is used to keep the machine model as close to reality as possible. Also the environmental models should be as close to reality as possible, therefore the Discrete Element Method, DEM, is used for the gravel pile model. From analysis of the power loss maps and the problem setup it can be shown that the problem is non-convex. In most of the commonly used optimal control solvers found in literature it would be troublesome to handle these data tables. This is mostly due to the fact that most of the solvers are gradient based. Thus if the optimization has a machine model that is map based, in practice the gradients can be tedious to calculate. Considering this and the desire to ensure that global optimum is found, an algorithm based on dynamic programming was developed by the author.

In discrete form the problem can be formulated as:

$$\begin{aligned} \underset{\boldsymbol{x_0}, \boldsymbol{u_0}, \boldsymbol{x_1}, \dots \boldsymbol{u_{N-1}}, \boldsymbol{x_N}}{\text{minimize}} \quad & \sum_{k=0}^{N-1} L(\boldsymbol{x_k}, \boldsymbol{u_k}) + \frac{\beta}{x_{k,1}} + E(\boldsymbol{x_N}) \\ \text{subject to} \quad & f(\boldsymbol{x_k}, \boldsymbol{u_k}) - \boldsymbol{x_{k+1}} = 0 \; for \; k = 0, \dots, N-1 \\ & \bar{\boldsymbol{x}}_{\boldsymbol{0}} - \boldsymbol{x_0} = 0 \\ & \bar{\boldsymbol{x}}_{\boldsymbol{N}} - \boldsymbol{x_N} = 0 \\ & \bar{x}_{TP,1} - x_{TP,1} = 0 \end{aligned} \tag{1}$$

Here $\boldsymbol{x_k}$ are the states, $\boldsymbol{u_k}$ are the control signals;

$\boldsymbol{x_{k,1}} = vehicle\ velocity \qquad \boldsymbol{u_{k,1}} = propulsion\ power$

$\boldsymbol{x_{k,2}} = lift\ cylinder\ position \qquad \boldsymbol{u_{k,2}} = lift\ cylinder\ velocity$

$\boldsymbol{x_{k,3}} = tilt\ cylinder\ position \qquad \boldsymbol{u_{k,3}} = tilt\ cylinder\ velocity$

at time k. In $L(\boldsymbol{x_k}, \boldsymbol{u_k})$ the energy usage per sample, which becomes the power in each sample to be minimized, is computed according to the simulation model presented in Section 5.3. β is a weighting factor that affects the cycle time by enforcing different average velocity of the wheel

loader. $E(\boldsymbol{x_N})$ are the terminal penalties for ensuring correct end conditions. In $f(\boldsymbol{x_k}, \boldsymbol{u_k})$ the states for the next sample are computed according to the simulation model presented in Section 5.3. $\bar{\boldsymbol{x}}_{\boldsymbol{0}}$ are the initial conditions and $\bar{\boldsymbol{x}}_{\boldsymbol{N}}$ are the end conditions. The initial and end conditions for all three states are set by the phase boundary conditions as explained in Section 5.2. $\bar{x}_{TP,1}$ is the turning point condition as shown in Figure 11. The states, $\boldsymbol{x_k}$, and the control signals, $\boldsymbol{u_k}$ are discrete sets limited by the physical limits of the components in the wheel loader.

5 Theoretical Global Optimum

An optimal control method, together with the related algorithms and implementation, that ensures global optimum, according to the set requirements, are presented in this chapter. The optimal control method and the model of the wheel loader and its environment have to be able to interact in a way that the computation time is kept reasonable. The model of the wheel loader and its environment, with limitations, are also presented in detail.

5.1 Optimal Control Method

Many optimal control methods are available, in literature such as [38] and [39]. In the recent decades, optimal control has become more popular, much due to the fact that available computational power has increased substantially, enabling the use of optimal control in more applied industrial areas. More recent literature that explains different optimal control methods and how to use them in modern computers are [40,41].

Different optimization methods can be used to compute a numerical theoretical optimum with regard to fuel efficiency in a vehicle. In [42], an on-road vehicle system optimization problem is investigated by performing a "convexification" of the problem. In [3] the transport part in a wheel loader work cycle is optimized, the optimal control problem solver PROPT [43] is used, which uses a pseudo-spectral collocation method to solve a formulated multi-phase optimal control problem. Dynamic programming is chosen in this paper according to the line of argument in Section 4.

5.1.1 Dynamic Programming

Dynamic programming is an optimal control method where exhaustive search is performed in a structured way [44].

Assuming that the work cycle geographical boundary constraints are set, the focus is then on the "*actuator optimization*" level in Figure 3. The optimization problem is to solve how the three actuators; propulsion, lift, and tilt, should behave to optimize the fuel efficiency during the work cycle, while ensuring that the desired work cycle time is achieved to keep the required productivity. This means that the problem has three control signals, $\boldsymbol{u_{k,1\ to\ 3}}$ in **(1)**. However, for visualization purposes a schematic "one control signal" case is shown in Figure 8.

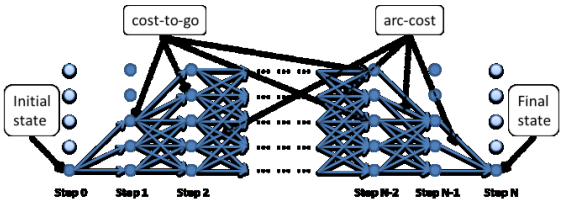

Figure 8 – Schematic example of a transition graph, for the forward computation, in a "one control signal" problem.

Dynamic programming is a discrete method based on taking a decision at every sample. The basic idea is to compute backwards, for a known work cycle, the cost-to-go in each discrete sample for each discretized state value in a first loop, and in that way get the optimal path. Then the control signals are extracted by the help of the arc-costs, which in this case relates to the energy consumed by the wheel loader during that step. Interpolation is used between the current cost-to-go and the sum of the previous cost-to-go and the arc costs to be able to keep a sparse grid to save computational power. In a given work cycle the discretization of the x-axis is the distance. There are three "y-axes"; wheel loader velocity, lift cylinder position and tilt cylinder position. This corresponds to the state $\boldsymbol{x_{k,1\ to\ 3}}$ in **(1)**. The initial and final machine positions are set so that the wheel loader completes the work cycle. The initial, $\bar{\boldsymbol{x}}_{\boldsymbol{0}}$, and final, $\bar{\boldsymbol{x}}_{\boldsymbol{N}}$, states are set according to the boundary conditions given in by the geographical boundary constraints imposed on the work cycle. This result in forbidden arc-costs, see the beginning and end in Figure 8. The control signals, $\boldsymbol{u_{k,1\ to\ 3}}$ in **(1)**; the electrical propulsion machine torque, the lift cylinder speed and the tilt cylinder speed all have limitations because of the physical limitations of the electrical machines, which results in a maximum possible acceleration. This is why not all transitions are allowed in the middle of the graph in in Figure 8. More about dynamic programming can be found in [44].

5.2 Dynamic Programming Implementation

An algorithm has been developed to find the global optimum with regards to fuel efficiency [ton/l] for a given work cycle and a given machine concept, converted to electrical actuator energy efficiency [ton/J]. The work cycle is divided into four phases; "*Loading*", "*Transport with load*", "*Unloading*" and "*Transport without load*", see Figure 11. This is possible because the work cycle has fixed start and end points where each phase starts and ends. In the example presented in this paper these fixed points are taken from the measurement. The computational time is lower when the phases are computed in parallel, and due to the fixed boundary points the split does not affect the optimization results. Dividing the problem into a path planning optimization of the work cycle and an actuator optimization adds a risk of sub-optimal solutions. However, in many cases these points are set by outer environmental constraints such as location of the pile, load receiver and other obstacles.

In dynamic programming, the implementation is a challenge due to the curse of dimensionality [39]. Furthermore, the level of discretization and the computation time are interrelated. To investigate how the discretization of the control signal affects the optimal control results, different runs with increasing control signal discretization have been performed, visualized by the blue crosses in Table 1. Only the control signal discretization matters since this sets the resolution in the output power for the three actuators. This in turn results in a motion, either on the driveline or the working hydraulics.

The total power of all three actuators with the cycle time weighting factor corresponds to the arc-costs in Figure 8.

Table 1 - Runs with different levels of discretization.

Run	Control signal discretization	State discretization	Marker
1	11x11x11	11x10x10	X
2	21x21x21	11x10x10	X
3	41x41x41	11x10x10	X
4	61x61x61	11x10x10	X
5	81x81x81	11x10x10	X
1	11x11x11	21x19x19	O
2	21x21x21	21x19x19	O
3	41x41x41	21x19x19	O

As can be seen in Figure 9, represented by the blue crosses, the normalized energy usage is relatively insensitive to control signal discretization increases past "Run" 2". With further discretization, the solution changes by less than 1%. Therefore this discretization level is used henceforth.

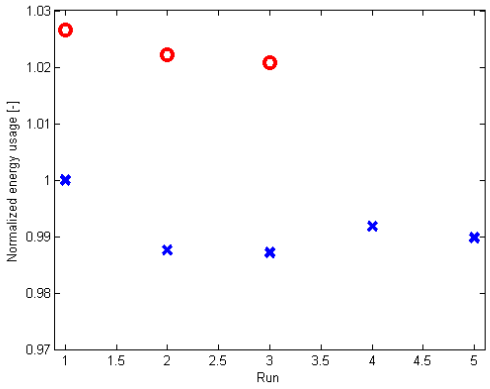

Figure 9 - Normalized energy usage for different discretization levels. Legend and level of discretization according to Table 1.

To investigate how sensitive the result is to the interpolation between the states, when interpolating from the different arc-costs, three of the simulations were repeated with an increased level of discretization of the states. The results are represented with red circles in Table 1. and Figure 9. The difference in the results of the two discretization levels is small in comparison to other sources of error, for example the simplified machine and environment model presented in Section 5.3. Considering the exponential increase in calculation time with each increasing level of discretization, see Figure 10, there is no practical justification for using a higher level of discretization. However, there are other ways to increase the level of accuracy, for example by using a better interpolation. A two-step interpolation calculation, in each sample, is used in the final version of the optimization algorithm which increases the accuracy, so that it will be used henceforth.

The calculation times for the different simulations in Table 1 are shown in Figure 10. Here the exponential curse of dimensionality is clear and the importance of keeping the discretization as low as possible are visible.

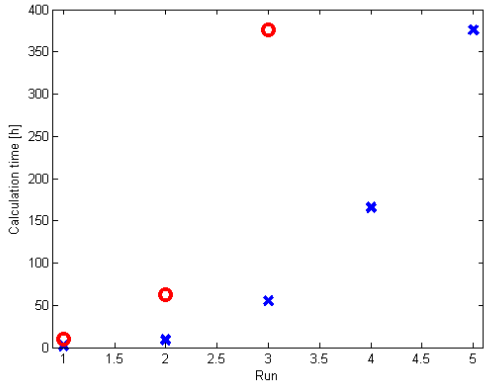

Figure 10 - Calculation times for simulations. Legend and level of discretization according to Table 1.

More about convergence of the dynamic programming algorithm is presented in [13].

To be able to reach the fixed points in the working cycle, end penalties, $E(\boldsymbol{x_N})$ in **(1)**, have to be implemented. These ensure that the wheel loader is moving and energy is used. A weighting factor, β in **(1)** and **(2)**, has to be implemented to ensure that the desired work cycle time is achieved.

To simplify the understanding, a pseudo-code of the implementation of the dynamic programming is shown in Code 1. The cost-to-go is first computed backwards to get the costs in all points in Figure 8 and ensure correct ending point.

```
for i=final discretized distance step
      down to 0
  for j=0 to top discretized machine
        velocity
    for k=lowest to highest discretized
         lift position
      for l=lowest to highest discretized
           tilt position
      Compute the arc-cost according to (2).
      Save cost-to-go in each grid point
        for use in Code 2 by accumulating
        the minimum arc-cost and previous
        cost-to-go.
      end
    end
  end
end
```

Code 1 – Pseudocode for the backward computation of the cost-to-go.

There is a high out of bound penalization factor implemented when calculating the arc cost to ensure that the algorithm keeps within the boundary conditions of the components. To reduce computational time whilst keeping the accuracy in the optimization, a method is used that decreases the discretization level and instead computes two steps inside every loop.

Then the algorithm computes forward, according to the pseudo-code in Code 2, from the correct starting point to find the control signals that result in the global optimal solution, with regard to energy efficiency of the actuators.

```
for ii=0 to final discretized distance
  Compute the arc-cost according to (2).
  Compute the total cost by adding arc-
    cost and cost-to-go from Code 1.
  The optimal control signals are derived
    from the minimum total cost.
end
```

Code 2 – Pseudocode for the forward computation, extracting the optimal control signals.

The arc-costs represent the sum of the energy consumption of all actuators in each arc computation and hence each distance step. The calculations of the arc-costs are detailed in Section 5.3.

The tool has also been developed to enable the investigation of the Pareto front that visualizes the trade-off between productivity and fuel efficiency, and forms the machine trade-off curve presented in [1]. This is done here by changing the cycle time penalty, β, and in that way calculating the maximum fuel efficiency for all the possible cycle times, which essentially corresponds to the productivity, given the load, for the wheel loader. This information can then be used to optimize a complete work site. When evaluating different complete machine concepts the machine trade-off curve, which is the trade-off between fuel efficiency and productivity, can differ, both with regard to maximum fuel efficiency at different productivity, and also the characteristics of the maximum fuel efficiency over the productivity range for the specific wheel loader. It is advantageous to have a machine trade-off curve as forgiving as possible to facilitate different operator behavior [1]. But also to have the most robust machine possible to enable different production rates at different customer sites while maintaining high energy efficiency. More details on multi-objective optimization can be found in [45,46].

5.3 Simulation Model

The model of energy usage, represented by the function, $L(x_k, u_k)$ in (1), consists of the wheel loader model and the model of its environment. The purpose is to calculate the power consumption as accurately as possible, since energy efficiency [ton/J] is the main optimization criteria.

The arc-cost in Code 1 and Code 2 is computed according to (2),

$$\boldsymbol{arc\_cost} = \left(\boldsymbol{P_{prop}} + \boldsymbol{P_{lift}} + \boldsymbol{P_{tilt}} + \boldsymbol{\beta}\right) \cdot \frac{\Delta s}{v_{avg}} \quad \textbf{(2)}$$

where P_{prop} is the propulsion power delivered to the driveline, P_{lift} is the lift power, P_{tilt} is the tilt power, β is weighting factor discussed in Section 5.2 and $\frac{\Delta s}{v_{avg}}$ is the time step converted according to (3).

$$\Delta t = \frac{\Delta s}{v_{avg}} \cdot \quad \textbf{(3)}$$

where Δt is the time step, v_{avg} is the average velocity of the wheel loader in the time step and Δs is the distance travelled in the time step.

The propulsion power is computed according to (4).

$$P_{prop} = P_{wheel} + P_{axle\_loss} + P_{gbx\_loss} + P_{eds\_loss} \quad \textbf{(4)}$$

where P_{wheel} is the power exerted on the wheels, P_{axle_loss} is the losses in the axles, P_{gbx_loss} is the gearbox losses and P_{eds_loss} is the losses in the propulsion electric drive system, which include the electrical machine and power electronics. The wheel power is computed from (5), (6), (8) and (9).

$$P_{wheel} = T_{wheel} \cdot \omega_{wheel} \quad \textbf{(5)}$$

where T_{wheel} is the torque exerted on the wheels and ω_{wheel} is the wheel speed. The wheel torque is computed from

$$T_{wheel} = F_{wheel} \cdot r_{wheel} \quad \textbf{(6)}$$

where r_{wheel} is the wheel radius and F_{wheel} is the force exerted from the wheels to the ground.

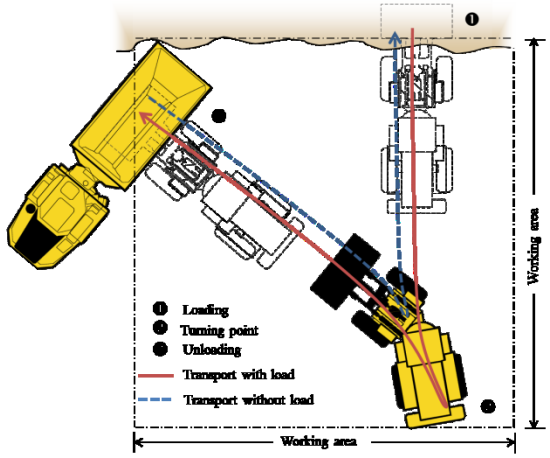

Figure 11 – Visualization of the "*short loading cycle*", showing the phases and working area, modified from [27].

In the loading phase, see Figure 11, the wheel force and the vehicle speed are determined in the gravel simulation model, represented by f_1 in (7), presented further in Section 5.4.1. The bucket trajectory is defined by the forward position, x_{bucket}, the upward position, y_{bucket} and the angle of the bucket, θ_{bucket}. This bucket trajectory is used as input to the DEM simulation.

$$(x_{bucket}, y_{bucket}, \theta_{bucket}) = f_1(F_{x\_bucket}, v_{x\_bucket}, F_{z\_bucket}, v_{y\_bucket}, T_{bucket}, \omega_{bucket}) \quad \textbf{(7)}$$

The results from the DEM simulations are then post processed via a Volvo internal kinematic model of the lifting unit represented by f_2 in (8).

$$\left(F_{wheel}, v_{avg}, F_{lift_{cyl}}, v_{lift_{cyl}}, F_{tilt_{cyl}}, v_{tilt_{cyl}}\right) = f_2(F_{x\_bucket}, v_{x\_bucket}, F_{z\_bucket}, v_{y\_bucket}, T_{bucket}, \omega_{bucket}) \quad \textbf{(8)}$$

where F_{x_bucket} is the force on the bucket, v_{x_bucket} is the velocity of the bucket, in the forward direction, F_{z_bucket} is the force on the bucket, v_{y_bucket} is the velocity of the bucket, in the upward direction, T_{bucket} is the torque on the bucket and ω_{bucket} is the angular velocity of the bucket, see Figure 12.

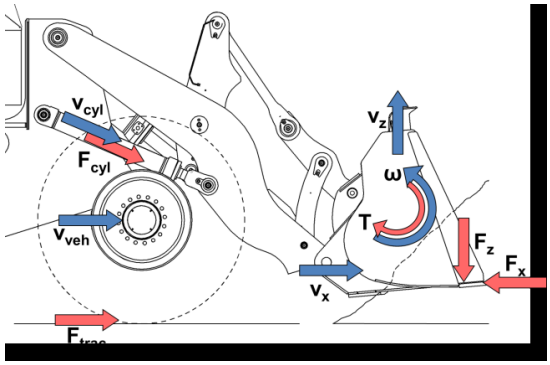

Figure 12 – Schematic picture of the forces and speeds of the bucket and how they translate to cylinder and vehicle forces and speeds, modified from [28].

In the rest of the work cycle, transporting and unloading, the wheel force results in an acceleration force for the vehicle according to the vehicle motion equation in (9) [32].

$$F_{acc} = F_{wheel} - F_{roll} - F_{air} \quad \textbf{(9)}$$

where, F_{acc} is the acceleration force for the vehicle, F_{roll} is the rolling resistance and F_{air} is the air resistance. F_{roll} is simplified to be constant since in the "*short loading cycle*" the working area is constrained to a small geographical area according

to Figure 11. The acceleration force generates the vehicle velocity, see (10), this is the state in the driveline.

If v_{final} is the end velocity for the discrete step, v_{init} is the initial velocity, m is the vehicle mass and Δs is the step distance, the resulting motion of the wheel loader can be computed as in (10).

$$v_{final} = v_{init} + \frac{F_{acc}}{m} \cdot \frac{\Delta s}{v_{init}} \quad (10)$$

The control signal in the driveline, the propulsion electrical machine torque, T_{em}, is computed in (11).

$$T_{em} = \frac{T_{wheel} + \frac{P_{axle\_loss}}{\omega_{axle}} + \frac{P_{gbx\_loss}}{\omega_{gbx}}}{gr_{gbx} \cdot gr_{axle}} \quad (11)$$

where gr_{gbx} and gr_{axle} are the gear ratios in the gearbox and axle. The mechanical losses in the gearbox and axles, P_{gbx_loss} and P_{axle_loss}, are computed in (12) and (13).

$$P_{gbx\_loss} = f_3(T_{wheel}, v_{avg}) \quad (12)$$

$$P_{axle\_loss} = f_4(T_{wheel}, v_{avg}) \quad (13)$$

where f_3 and f_4 are tabulated values from test rig measurements.

The losses in the electric drive system, P_{eds_loss}, are computed in (14).

$$P_{eds\_loss} = f_5(T_{em}, \omega_{em}) \quad (14)$$

where ω_{em} is the speed of the propulsion electrical machine and f_5 consists of tabulated values from test rig measurements.

The power to the hydraulic system, P_{lift} and P_{tilt} is computed by (15) and (16).

$$P_{lift} = f_6(F_{lift\_cyl}, v_{lift\_cyl}) \quad (15)$$

$$P_{tilt} = f_7(F_{tilt\_cyl}, v_{tilt\_cyl}) \quad (16)$$

where F_{lift_cyl} and F_{tilt_cyl} are the forces on the lift and tilt cylinder. v_{lift_cyl} and v_{tilt_cyl} are the velocities of the lift and tilt cylinder. This is the control signal for the hydraulic actuators. The functions f_6 and f_7 are tabulated values from test rig measurements.

In the loading phase, see Figure 11, the cylinder forces and velocities are determined in the DEM gravel simulation via a Volvo internal kinematic model of the lifting unit in the same way as the propulsion; see (7) and (8). In the rest of the work cycle, transporting and unloading, the cylinder forces are computed in (17).

$$(F_{lift\_cyl}, F_{tilt\_cyl}) = f_8(pos_{lift\_cyl}, pos_{tilt\_cyl}) \quad (17)$$

where pos_{lift_cyl} and pos_{tilt_cyl} are the cylinder positions, which are the states for the hydraulic system, and f_8 is derived from the Volvo internal kinematic model of the lifting unit.

The wheel loader model is described by equations (8), (11) to (17) and is built of quasi-static power loss maps for each component that originate from real test rig measurements. The maps correspond to f_2 to f_8 in the equations. Maps are an accurate way to model the wheel loader because the true, measured losses are accounted for and good opportunities for analysis of the different major sub-systems are possible. All the major components are included: in the driveline; wheels, axles, transmission, electrical machine and power electronics and for the working hydraulics; lifting unit, hydraulic cylinder, hydraulic machine, electrical machine and power electronics. Furthermore, indexed search in the maps enables fast computations.

5.4 Trajectory Generation

Figure 13 shows the simulation process employed: the bucket trajectories, generated in MathCad or Matlab, have been transferred as text files to the DEM particle simulation run in Pasimodo, as reported in [33]. The results have been transferred back to MathCad for post processing, for example converting the forces acting on the bucket into cylinder forces and rim pull demand. The results are then either passed on to Matlab and the optimal control algorithm running the wheel loader simulations or kept within MathCad to compute the simple performance indicators published in [5].

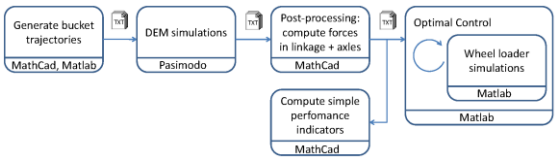

Figure 13 – Workflow for calculating the numerical theoretical global optimum, including the trajectory generation process [48].

The MathCad parts in this process could just as well have been performed in Matlab too. In the aftermath of this work, all scripts and the toolbox developed for such calculations, have in fact been ported to Matlab.

Ideally the DEM simulation would be part of the overall simulation that includes the optimal control calculations. In this way, both physical properties and optimality would be ensured. However, no traditional optimal control algorithm can be used as the overall problem is not, and cannot, be made convex. This in turn precludes the use of gradient descent optimization. Instead the proposed algorithm based on dynamic programming may be used. However, running one big simulation with a complex machine model in a sufficiently detailed environment, controlled by an adaptive operator model is impossible with the calculation resources typically available today, because the computational costs using dynamic programming would be extraordinary high. This can of course change in the near future, considering cloud computing [48].

The forces on the bucket at a given point in a trajectory through the pile are highly dependent on the history of where the bucket has been in past time samples. This means that if dynamic programming is to be used in the "*Loading*" phase then at each discrete time step, when a decision is to be taken about whether the bucket should be lifted, tilted or penetrate the pile further, the complete trajectory has to be recalculated in the DEM gravel pile model. This co-simulation would require excessive computation power and computation time. Instead a dynamic programming inspired brute force exhaustive search of all possible trajectories through the pile was done. This works by simulating, in the DEM gravel pile model, as many trajectories as possible that are in the viable region, where the wheel loader can perform the trajectory, and then use these ready simulated trajectories in the dynamic programming framework that is used in the "*Transport with load*", "*Unloading*" and "*Transport without load*" phases. The reason for using the dynamic programming framework and not only an exhaustive search is that the end-positions of the lift and tilt are not the same in all the trajectories resulting in different input to the "*Transport with load*" phase.

Two methods have been used to create the trajectories that were simulated in the DEM gravel pile model. First a set of trajectories were created using recursive programming [47] by discretizing the three actuators and moving one, two or three of the actuators one discrete step during each time sample, see the blue trajectories in Figure 14. At the desired discretization level, several hundred thousand trajectories would need to be simulated in DEM, which is not feasible due to computation time. A lower discretization level was chosen [48] in the recursive programming instead. Additionally and a set of analytical trajectories were created manually as a complement, see the red trajectories in Figure 14. The analytically created trajectories are motivated by engineering experience of different bucket filling strategies observed from professional operators [33]. All trajectories are simulated in the DEM gravel pile model. Altogether 5781 trajectories were simulated on a cluster of 800 CPU-cores, taking a week to calculate in 2013.

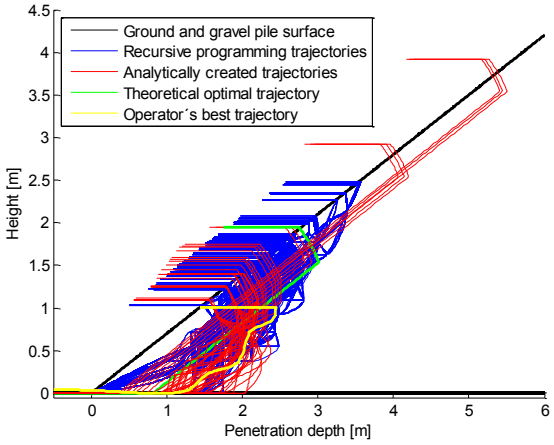

Figure 14 - Simulated bucket fill trajectories in DEM. The bucket tip trajectory is drawn. The black lines are the ground level and gravel pile surface. The blue trajectories originate from the recursive programming and the red from the analytically created trajectories. The green trajectory is the numerical theoretical optimal trajectory and the yellow is the trajectory of the best empirically found operator from Figure 6.

The global optimum trajectory has to be calculated together with the complete work cycle, as have been proved in [48]. This is done in the dynamic programming framework presented in Section 5.2. The optimum trajectory can be guaranteed to be global with respect to the level of discretization in the recursive programming. Due to the fact that there is no analytical solution the optima will always depend on the discretization level.

5.4.1 Discrete Element Method

To compute the arc-cost in the loading phase, consequently the energy, the forces acting on the bucket during loading must be known. The bucket is modeled as a rigid body interacting with the gravel pile. Many ways for modeling gravel can be seen in literature, often by simplified models that are computationally fast but are not that accurate at calculating the bucket forces [49,50]. An attempt to

combine the two methods of "simplified gravel piles" and "Discrete Element Method" can be found in [51], however obtaining the correct forces seems to be a challenge. The decision was made to use the more accurate gravel pile simulation method DEM, Discrete Element Method, that has proven to be a reliable method of modeling gravel and cohesionless soil [52,53].

In the DEM, the gravel pile consists of discrete particles that interact with each other through a simplified contact law. Two particles are allowed to slightly overlap and a repulsive force proportional to the overlap pushes particles apart according to (18).

$$\mathrm{F}_n = k_n \cdot \delta_{ij} + d_n \cdot \dot{\delta}_{ij} \quad \textbf{(18)}$$

where, δ_{ij} is the overlap between two particles indexed by i and j. k_n is the normal stiffness coefficient and d_n is the damping parameter. It becomes possible to formulate a scale invariant model by correlating the normal stiffness to the Young's modulus of the material [54,55].

The majority of the draft forces acting on the bucket are caused by inter-particle friction. In the following, the model for Coulomb friction is outlined. Once two particles are in contact, the contact points $\mathbf{x}_i$ and $\mathbf{x}_j$ on both particles are stored, as well as a contact normal $\mathbf{n}$ that is orthogonal to the surfaces of the two particles. As soon as the particles move, the relative position of the contact points is projected onto a plane orthogonal to $\mathbf{n}$ to obtain the tangential deformation vector according to (19).

$$\boldsymbol{\xi}_t = \mathbf{n}\cdot(\mathbf{x}_i - \mathbf{x}_j) \quad \textbf{(19)}$$

The tangential force $\mathbf{F}_t$ is computed in (20).

$$\mathbf{F}_t = k_t \cdot \boldsymbol{\xi}_t + d_t \cdot \dot{\boldsymbol{\xi}}_t, \quad \textbf{(20)}$$

where k_t and d_t are the tangential stiffness and damping parameters respectively. If the magnitude of the calculated tangential force is greater than the Coulomb limit $\mu \cdot \mathrm{F}_n$, the contact is in sliding mode. In this case, the tangential force is clamped to the Coulomb limit, i.e. $\mathbf{F}_t = \mu \cdot \mathbf{F}_n$, and the deformation vector is updated according to (21).

$$\boldsymbol{\xi}_t^* = \frac{\mu \cdot \mathrm{F}_n}{k_t} \cdot \frac{\xi_t}{\|\xi_t\|} \quad \textbf{(21)}$$

If $\mathbf{q}_i$ and $\mathbf{q}_j$ are the centers of mass of the two particles respectively, $\mathbf{x}_a = \mathbf{q}_i + \frac{\mathbf{r}_i}{\mathbf{r}_i+\mathbf{r}_j} \cdot (\mathbf{q}_i+\mathbf{q}_j)$ is called the actuation point of the contact. The contact points on the particles are updated to $\mathbf{x}_i = \mathbf{x}_a + \frac{\xi_t^*}{2}$ and $\mathbf{x}_j = \mathbf{x}_a - \frac{\xi_t^*}{2}$ and stored in the local coordinate systems of the particles for use in the next time step. The tangential force is recalculated accordingly. As a result, the particles are in sliding mode.

While DEM allows for many complex contact models, the simple normal and tangential contact models introduced here suffice for the purpose of measuring draft forces in dry gravel [33,53]. Dry gravel is used to be able to compare with the measurements done inside the tent, see Figure 5.

Once the contact forces are known, they can be explicitly integrated to obtain the velocities and positions of all particles in the gravel pile. The contact forces resulting from contacts between particles and the bucket of the wheel loader are used to compute the arc-cost of the loading phase.

The simulation setup is identical to the one in [33]. The gravel pile is 5m high, see Figure 15. To save computational cost, a 1m wide slice of the pile is used in the simulation. The forces on the bucket are then corrected via an appropriate weighting factor according to the width of the bucket. Comparisons to a full three dimensional simulation were performed to make sure this is a reasonable simplification. The slice of the gravel pile consists of approximately 16,000 spherical non-rotational particles. The material parameters are chosen according to a known material that has previously been parameterized with the help of laboratory tests.

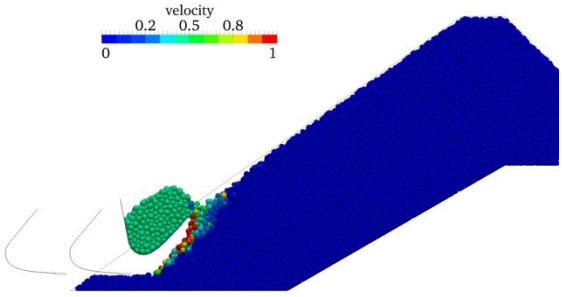

Figure 15– Snapshots of a DEM simulation using a 5m high, 1m wide gravel pile.

6 Comparison Analysis

To be able to compare the numerical theoretical optimum with measurements in a fair manner, the fuel efficiency in the measured trajectories has to be computed backwards through the same machine model and environmental model as is used in the optimization. The cycle used for comparison is shown in Figure 14 and Figure 16. To ensure that it is valid to compare the operator behavior in the larger empirical study, which is performed on a conventional wheel loader, with a new machine concept, such as the precursor [36] to the recently revealed concept wheel loader "LX1" [37], a smaller set of measurements, done on the machine concept in the optimization algorithm is considered as well. The smaller set of measurements, done only on a couple of operators, performing a handful of work cycles each show the same pattern as in Figure 6, but with fewer data points.

7 Results

The main result is that the optimal control algorithm, based on dynamic programming, works. The result shows about 14% better energy efficiency than the best work cycle that could be found empirically. The best measured work cycle is around 30% better than the average in the measurement. The trajectories for the three actuators; propulsion, lift and tilt, in the full work cycle comparison are shown in Figure 16 together with the accumulated energy, the operator trajectories in dashed blue and the optimal control result in solid black.

The small differences in initial vehicle speed, hinge pin height and attachment angle in Figure 16 is due to the simulation setup of the gravel pile simulations discussed in Section 5.4. The final vehicle speed, hinge pin height and attachment angle is adjusted to have the same offset as the initial values.

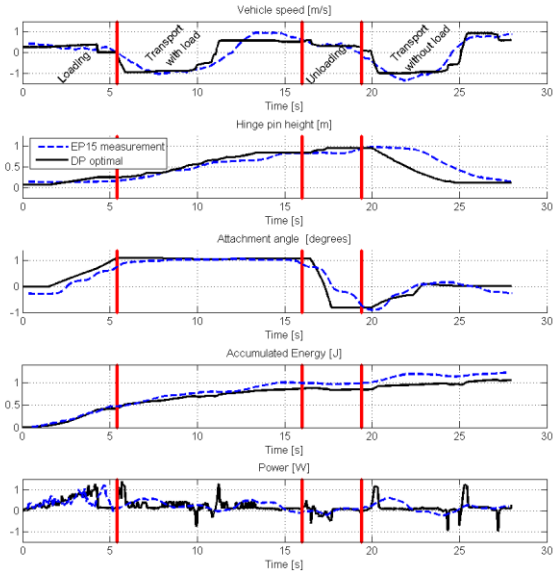

Figure 16– Actuator comparison between the best operators' most fuel efficient cycle in Figure 6, dashed blue line, and the optimal solution, solid black line. Hinge pin height is computed from lift cylinder position and attachment angle is computed from tilt cylinder position. Normalized axes due to Volvo internal results.

The 14% energy efficiency gain, in Figure 16, is fairly distributed throughout the cycle. The energy used by the operator and the optimal control algorithm is compared in each phase to find the energy saving contribution per phase. The result is shown in Table 2.

Table 2 – Energy efficiency gain in each phase and the energy efficiency gain distribution per phase for the complete work cycle in Figure 16.

	Efficiency gain	Efficiency gain distribution
Loading	10%	28%
Transport with load	15%	44%
Unloading	79%	9%
Transport without load	14%	19%
Complete work cycle	14%	100%

In the loading phase, the numerical theoretical optimal solution slices through the pile while the best operator keeps on pushing into the pile at the end of the bucket filling phase, as can be seen in Figure 14 and Figure 16. The optimal control solution avoids the last push, where high power is needed, but not that much more material ends up in the bucket, therefore the optimal control solution needs less force than the best operator found in Section 2. The optimal bucket filling strategy is fully investigated and explained further in [48]. In the transport phases the majority of the savings

come from hard acceleration and deceleration and keeping a low constant speed longer rather than accelerating and decelerating slowly during the complete transport, sees Figure 16. The gain is higher in the transport with load due to higher gross vehicle mass and simultaneous lifting. In the unloading phase the reasons are similar to the travel phase, however with more focus on the tilt out function. The actuators, mostly tilt in this case, are used closer to the optimum working point, which in this case means tilting at higher constant speed. The fuel efficiency gain distribution is highly dependent on the work cycle and the operator. More detailed studies on more operators, comparing to the optimum are presented in [24].

8 Discussion

A secondary result is that the optimal control algorithm is ready to be used as input to operator assist systems, automatic functions and autonomous construction machine control [24]. Once the DEM simulations have been simulated in advance they can be used as a library, then the computation time for the optimization takes around 4 hours on a laptop. This is of course not feasible to implement in an on-board ECU today. Rather the lessons learnt from the optimal control results have to be used to develop, for example, a fast heuristic controller that can help the operator in an operator assist system or in automatic functions and autonomous construction machine control.

Another secondary result is that the optimal control algorithm can be used in a concept evaluation, between different hybrid wheel loader concepts for example, and system optimization, with regard to components sizes, for each individual concept. This has been done in [21]. In concept evaluation and system optimization the computation time, 4 hours, is not that significant. The computations are easily parallelized. This means that on eight cores and one week a batch of 336 machine setups can be simulated, which is acceptable.

Due to the fact that a prediction of the exact properties of the gravel pile, and the fact that many of the savings comes from harsh accelerations and decelerations in the other phases, it is estimated that a gain of around 10% energy efficiency should be possible in a real-world production chain wheel loader in a bucket application. Depending on the amount of operator assistance, the 10% can shift a bit up and down. In an operator only scenario, with only operator training, it can be as low as 5% higher fuel efficiency, while in a full autonomous wheel loader where harsh accelerations and decelerations do not matter since there is no operator in the machine, the fuel efficiency could be well over 10% higher than the best manually operated wheel loader.

Further validation is needed regardless of whether the results from the method presented in this paper are to be used as: input to operator assist systems; automatic functions and autonomous construction machine control; or in early development phases, performing system optimization and concept evaluation. For a complete evaluation of the algorithm, before it is used in production, many more work cycles and applications have to be analyzed. This ensures that cycle-beating does not occur. This is even more important in off-road than in on-road applications because many working machines, such as the wheel loader, operate in a vast variety of environments. If cycle-beating is not considered, the wheel loader manufacturer can end up with a machine that performs excellently in some applications but underperforms in other.

9 Conclusions

The main challenge when optimizing actuator trajectories in a complete work cycle of a wheel loader in bucket applications is the extensive computation power needed to calculate the bucket-soil interaction in the bucket fill phase.

The optimal control method and the implemented algorithms presented in this paper finds a numerical theoretical global optimum that has 14% higher fuel efficiency comparing to the most fuel efficient operator's best work cycle found empirically. Since the best operator is about 30% more fuel efficient than the fleet average, in the empirical study, the potential for using the optimal control results on a larger fleet of operators could be in the range of 40-45%. This is dependent on the operator and application according to the measurements in the empirical study in Section 2. The algorithm can be used to optimize productivity, or a combination of fuel efficiency and productivity, as well.

The optimal control results can be used as input to operator assist systems, automatic functions and autonomous construction machine control.

The algorithm can serve as a tool in early development phases when performing concept

evaluations and system optimizations on new machine concepts. Using the method presented will minimize the dependency on control engineer experience, development time, operator deviations and test repeatability.

10 References

(Internet links verified 2018-01-29)

[1] Frank, B., Skogh, L., Alaküla, M., "On wheel loader fuel efficiency difference due to operator behaviour distribution". Proceedings of the 2nd Commercial Vehicle Technology Symposium (CVT2012), Kaiserslautern, Germany, March 13-15, 2012, pp 329-346, Berns, K. (ed.), Schindler, C. (ed.), Dreßler, K. (ed.), Jörg, B. (ed.), Kalmar, R. (ed.), Zolynski, G. (ed.). ISBN: 978-3-8440-0798-5.

[2] Nezhadali, V., Frank, B., Eriksson, L. "Wheel loader operation-Optimal control compared to real drive experience". Control Engineering Practice, Volume 48, Pages 1–9, March 2016. DOI: https://doi.org/10.1016/j.conengprac.2015.12.015

[3] Nezhadali, V., Eriksson, L., Fröberg, A., "Modeling and optimal control of a wheel loader in the lift-transport section of the short loading cycle", 7th IFAC Symposium on Advances in Automotive Control AAC 2013 Tokyo, Japan, 4–7 September 2013. In IFAC Proceedings Volumes, Volume 46, Issue 21, pp 195-200, 2013. Kawabe, T. (ed.). ISBN: 9783902823489 DOI: https://doi.org/10.3182/20130904-4-JP-2042.00083

[4] Backas, J., Ghabcheloo, R., Tikkanen, S., Huhtala, K., "Fuel optimal controller for hydrostatic drives and real-world experiments on a wheel loader", International Journal of Fluid Power", 17:3, 187-201, 2016. DOI: https://doi.org/10.1080/14399776.2016.1202081

[5] Filla, R., "Evaluating the efficiency of wheel loader bucket designs and bucket filling strategies with non-coupled DEM simulations and simple performance indicators", Fachtagung Baumaschinentechnik, September 16-17 2015, Dresden, Germany, 2015. DOI: https://doi.org/10.13140/rg.2.1.1507.1201

[6] Johannesson, L: "Predictive Control of Hybrid Electric Vehicles on Prescribed Routes". Department of Signals and Systems, Chalmers University of Technology, Göteborg, Sweden, 2009. ISBN: 978-91-7385-263-0

[7] Ottosson, J., "Energy Management and Control of Electrical Drives in Hybrid Electrical Vehicles". Department of Industrial Electrical Engineering and Automation, Lund University, Sweden, 2007. ISBN: 978-91-88934-46-8

[8] Larsson, V., "Route Optimized Energy Management of Plug-in Hybrid Electric Vehicles" Chalmers University of Technology, Göteborg, Sweden, 2014. ISBN: 978-91-7597-002-8

[9] Hung, C-W., Vu, T-V., Chen, C-K., "The Development of an Optimal Control Strategy for a Series Hydraulic Hybrid Vehicle", Applied Sciences 6, no. 4: 93, 2016. Lin, C. J. (ed.) DOI: https://doi.org/10.3390/app6040093

[10] Molla, S., Ayalew, B., "Power management strategies for a Series hydraulic hybrid drivetrain", International Journal of Powertrains, Vol. 1, No. 1, pp.93–116, 2011. DOI: https://doi.org/10.1504/IJPT.2011.041911

[11] Wu, B., Lin, C-C., Filipi, Z., Peng, H., "Optimal power management for a hydraulic hybrid delivery truck", International Journal of Vehicle Mechanics and Mobility, Vol. 42, Nos. 1-2, pp. 23–40, 2004. DOI: https://doi.org/10.1080/00423110412331291562

[12] Nilsson, T., "Optimal Predictive Control of Wheel Loader Transmissions", Linköping University, Sweden,ISBN: 978-91-7519-171-3, 2015.

[13] Frank, B., Fröberg, A., "Establishing an Optimal Work Cycle for an Alternative Wheel Loader Concept". Proceedings of the International Exposition for Power Transmission (IFPE2014) , ch 11.1., Las Vegas, USA, March 4-8, 2014, ISBN: 0-942220-49-8, 2014.

[14] Zimmerman, J., Hippalgaonkar, R., Ivantysynova, M., "Optimal Control for the Series-Parallel Displacement Controlled Hydraulic Hybrid Excavator", ASME 2011 Dynamic Systems and Control Conference and Bath/ASME Symposium on Fluid Power and Motion Control , Volume 1, Paper No. DSCC2011-5996, pp. 129-136, Arlington, Virginia, USA, October 31–November 2, 2011. ISBN: 978-0-7918-5475-4, DOI: https://doi.org/10.1115/DSCC2011-5996

[15] Hippalgaonkar, R., Ivantysynova, M., Zimmerman, J., "Fuel savings of a mini-excavator through a hydraulic hybrid displacement controlled system", 8th International Conference on Fluid Power (IFK), Dresden, Germany, March 26-28, 2012. https://www.researchgate.net/publication/282650613_Fuel_savings_of_a_mini-excavator_through_a_hydraulic_hybrid_displacement_controlled_system

[16] Wang, F., Zulkefli, M. A. M., Sun, Z., & Stelson, K. A., "Investigation on the energy management strategy for hydraulic hybrid wheel loaders", ASME 2013 Dynamic Systems and Control Conference, Volume 1: Aerial Vehicles; Aerospace Control; Alternative Energy; Automotive Control Systems; Battery Systems; Beams and Flexible Structures; Biologically-Inspired Control and its Applications; Bio-Medical and Bio-Mechanical Systems; Biomedical Robots and Rehab; Bipeds and Locomotion; Control Design Methods for Adv. Powertrain Systems and Components; Control of Adv. Combustion Engines, Building Energy Systems, Mechanical Systems; Control, Monitoring, and Energy Harvesting of Vibratory Systems, Palo Alto, California, USA, October 21–23, 2013 ASME 2013 Dynamic Systems and Control Conference, DSCC 2013 (Vol. 1). [V001T11A005] American Society of Mechanical Engineers (ASME), 2013. ISBN: 978-0-7918-5612-3 DOI: https://doi.org/10.1115/DSCC2013-3949

[17] Shen, W., Jiang, J., Su, X., Karimi, R H., "Control strategy analysis of the hydraulic hybrid excavator", Journal of the Franklin Institute, Volume 352, Issue 2, Pages 541-561, ISSN 0016-0032, 2015. DOI: https://doi.org/10.1016/j.jfranklin.2014.04.007

[18] Ohlsson-Öhman, K., "Identifying operator usage of wheel loaders utilizing pattern recognition techniques", Linköping University, Sweden, ISRN LiTH ISY EX 12/4591 SE, 2012. http://liu.diva-portal.org/smash/get/diva2:537110/FULLTEXT02.pdf

[19] Filla, R., "Optimizing the trajectory of a wheel loader working in short loading cycles", 13th Scandinavian International Conference on Fluid Power (SICFP'13), Linköping, Sweden, June 3-5, 2013. http://www.ep.liu.se/ecp/092/030/ecp13092030.pdf

[20] Nezhadali, V., Eriksson, L., "Optimal lifting and path profile for a wheel loader considering engine and turbo limitations", Optimization and Optimal Control in Automotive Systems, Lecture Notes in Control and Information Sciences, vol 455. Springer, Cham, 2014. Waschl, H. (ed.), Kolmanovsky, I. (ed.), Steinbuch M. (ed.), del Re L. (ed.). ISBN: 978-3-319-05370-7. DOI: https://doi.org/10.1007/978-3-319-05371-4_18

[21] Frank, B., "Using Optimal Control in Concept Evaluation and System Optimization of Diesel-Electric Hybrid Construction Machines" 4th International Conference on Electrical Systems for Aircraft, Railway, Ship propulsion and Road Vehicles & International Transportation Electrification Conference (ESARS ITEC 2016), Toulouse, France, November 2-4, 2016. ISBN: 978-1-5090-0815-5. DOI: https://doi.org/10.1109/ESARS-ITEC.2016.7841323

[22] Casoli, P., Gambarotta, A., Pompini, N., Riccò, L., ”Hybridization methodology based on DP algorithm for hydraulic mobile machinery - Application to a middle size excavator”, Automation in Construction, Volume 61, Pages 42-57, January 2016. DOI: https://doi.org/10.1016/j.autcon.2015.09.012

[23] Chauvin, A., Sari, A., Hijazi, A., Bideaux, E., ”Optimal sizing of an energy storage system for a hybrid vehicle applied to an off-road application”, 2014 IEEE/ASME International Conference on Advanced Intelligent Mechatronics (AIM) Besançon, France, July 8-11, 2014. DOI: https://doi.org/10.1109/AIM.2014.6878173

[24] Frank, B., “Utilizing Optimal Control and Physical Measurements when Developing Operator Assist, Automatic Functions and Autonomous Machines”, 6th IEEE International Conference on Control System, Computing and Engineering (ICCSCE 2016), Batu Ferringhi, Penang, Malaysia, November 25-27, 2016. DOI: https://doi.org/10.1109/ICCSCE.2016.7893555

[25] Nurmi, J, Mattila, J, “Global Energy-Optimal Redundancy Resolution of Hydraulic Manipulators: Experimental Results for a Forestry Manipulator” Energies, vol 10, no. 5:647, 2017. Vacca, A. (ed.). DOI: https://doi.org/10.3390/en10050647

[26] Nurmi, J., Mattila, J., “Global energy-optimised redundancy resolution in hydraulic manipulators using dynamic programming”, Automation in Construction, Volume 73, pp. 120-134, January 2017. DOI: https://doi.org/10.1016/j.autcon.2016.09.006

[27] Filla, R., “Quantifying Operability of Working Machines”, Linköping University, Sweden, ISBN 978-91-7393-087-1, 2011.

[28] Filla, R., “Operator and Machine Models for Dynamic Simulation of Construction Machinery”, Linköping University, Sweden, ISBN 91-85457-14-0, 2005.

[29] Kaneko, S., Ikimi, T., Moriki, H., Ito, N., Yanagimoto, H. “Patent Application: US20130151055A1”, 2013. https://patents.google.com/patent/US20130151055A1/en

[30] Bennik, C. “Wheel Loader Production Tips” http://www.forconstructionpros.com/article/10299484/wheel-loader-production-tips, 2006.

[31] VOLVO CONSTRUCTION EQUIPMENT Media Library, http://images.volvoce.com/#1516039372295_0.

[32] Guzzella, L., Sciarretta, A., “Vehicle Propulsion Systems - Introduction to Modeling and Optimization”, 2nd Edition, Softcover ISBN: 978-3-642-09415-6, Springer-Verlag Berlin Heidelberg, 2007.

[33] Filla, R., Obermayr M., Frank., B. “A study to compare trajectory generation algorithms for automatic bucket filling in wheel loaders”, 3rd Commercial Vehicle Technology Symposium (CVT2014), Kaiserslautern, Germany, March 11-13, 2014. Berns, K. (ed.), Schindler, C. (ed.), Dreßler, K. (ed.), Jörg, B. (ed.), Kalmar, R. (ed.), Zolynski, G. (ed.). ISBN: 9783844025736.

[34] Fu, J., “Logistics of Earthmoving Operations”, KTH Royal Institute of Technology, Sweden, 2013. ISBN: 978-91-87353-05-5.

[35] Rylander, D., “Productivity Improvements in Construction Site Operations Trough Lean Thinking and Wireless Real-Time Control”, Mälardalens University, Sweden, 2014. ISBN: 978-91-7485-173-1.

[36] Stein, G., Fröberg, A., Martinsson, J., Brattberg, B., Filla, R., Unnebäck, J., ”Fuel efficiency in construction machines – optimize the machine as a system”, 7th AVL International Commercial Powertrain Conference Proceedings, Graz, Austria, May 22-23, 2013-3.3, 2013. ISBN: 978-0-7680-8156-5. DOI: https://doi.org/10.13140/RG.2.1.2031.4089.

[37] Press release, http://www.volvoce.com/global/en/this-is-volvo-ce/what-we-believe-in/innovation/lx1-and-hx1/

[38] Bryson, A., Ho, Y., “Applied Optimal Control: Optimization, Estimation and Control”, ISBN-13: 000-0891162283, 1975.

[39] Bellman, R., “Dynamic Programming”, 2010, originally published 1957. ISBN: 9780691146683

[40] Diehl, M., Gros, S., “Numerical Optimal Control - (preliminary and incomplete draft)”, May 17, 2017. https://www.syscop.de/files/2017ss/NOC/script/book-NOCSE.pdf

[41] Betts, J.T., “Practical Methods for Optimal Control Using Nonlinear Programming”, 2nd edition, 2010. ISBN: 978-0-89871-688-7.

[42] Pourabdollah, M., “Optimization of Plug-in Hybrid Electric Vehicles”, Chalmers University of Technology, Sweden, ISBN: 978-91-7597-149-0, 2015.

[43] PROPT, ”http://www.tomdyn.com/”, tomlab 7.9.

[44] Bertsekas, D., ”Dynamic programming and optimal control”, vol 1-2, (Two-volume set), 2007. ISBN: 1-886529-08-6.

[45] Miettinen, K., ”Nonlinear Multiobjective Optimization”, fourth printing 2004.ISBN 0-7923-8278-1.

[46] Marler, R.T., Arora, J.S., ”Survey of multi-objective optimization methods for engineering”, Structural and Multidisciplinary Optimization, Volume 26, Issue 6, pp 369-395, April 2004. DOI: https://doi.org/10.1007/s00158-003-0368-6

[47] http://www.cs.utah.edu/~germain/PPS/Topics/recursion.html

[48] Filla, R., Frank, B. “Towards Finding the Optimal Bucket Filling Strategy Through Simulation”, 15th Scandinavian International Conference on Fluid Power – Fluid Power in the Digital Age (SICFP’17), Linköping, Sweden, June 7-9, 2017. https://www.iei.liu.se/flumes/sicfp17/Papersandpresentations/1.723022/sicfp2017_nonreviewed_Filla_Towards_Finding.pdf

[49] Svensson, H., ”Gravel pile model verification”, Volvo Construction Equipment internal technical report, Eskilstuna, Sweden,2012.

[50] Ericsson, A., Slättengren, J., “A model for predicting digging forces when working in gravel or other granulated material”, 15th ADAMS European Users Conference, Rome, October 4, 2000. http://citeseerx.ist.psu.edu/viewdoc/download?doi=10.1.1.504.6993&rep=rep1&type=pdf

[51] Yoshida, T., Koizumi, T., Tsujiuchi, N., Jiang, Z. et al., "Digging Trajectory Optimization by Soil Models and Dynamics Models of Excavator", SAE International Journal Commercial Vehicles 6(2), pp: 429-440, 2013. DOI: https://doi.org/10.4271/2013-01-2411.

[52] Obermayr M., Vrettos C., Kleinert J., et al. ”A discrete element method for assessing reaction forces in excavation tools”, Congress on Numerical Methods in Engineering (CNM 2013), Bilbao, Spain, June 28-28, 2013. http://publica.fraunhofer.de/documents/N-241440.html

[53] Obermayr M., Dressler .K, Vrettos, C., Eberhard P., ”Prediction of draft forces in cohesionless soil with the discrete element method“, Journal of Terramechanics, Volume 48, Issue 5, pp: 347-358 48, October 2011. DOI: https://doi.org/10.1016/j.jterra.2011.08.003.

[54] Obermayr, M., Dresser K., Vrettos C., et al, ”A bonded-particle model for cemented sand“, Computers and Geotechnics, Volume 49, pp: 299-313, April 2013. DOI: https://doi.org/10.1016/j.compgeo.2012.09.001.

[55] Ergenzinger C., Seifried R., Eberhard P., “A discrete element model to describe failure of strong rock in uniaxial compression“, Granular Matter, Volume 13, Issue 4, pp: 341-364, August 2011. DOI: https://doi.org/10.1007/s10035-010-0230-7.